

InstantRetouch: Personalized Image Retouching without Test-time Fine-tuning Using an Asymmetric Auto-Encoder

Temesgen Muruts Weldengus¹ Binnan Liu¹ Fei Kou² Youwei Lyu² Jinwei Chen²
 Qingnan Fan^{2†} Changqing Zou^{1,3†}

¹Zhejiang University ²vivo Mobile Communication Co. Ltd ³Zhejiang Lab

tememuruts@zju.edu.cn qingnanfan@vivo.com changqing.zou@zju.edu.cn

Abstract

Personalized image retouching aims to adapt retouching style of individual users from reference examples, but existing methods often require user-specific fine-tuning or fail to generalize effectively. To address these challenges, we introduce **InstantRetouch**, a general framework for personalized image retouching that instantly adapts to user retouching styles without any test-time fine-tuning. It employs an asymmetric auto-encoder to encode the retouching style from paired examples into a content disentangled latent representation that enables faithful transfer of the retouching style to new images. To adaptively apply the encoded retouching style to new images, we further propose Retrieval-Augmented Retouching (RAR), which retrieves and aggregates style latents from reference pairs most similar in content to the query image. With these components, **InstantRetouch** enables superior and generic content-aware retouching personalization across diverse scenarios, including single-reference, multi-reference, and mixed-style setups, while also generalizing out of the box to photorealistic style transfer.

1. Introduction

Image retouching enhances photographs to improve aesthetics or convey a specific narrative, but it is an inherently subjective task [20, 34], with user preferences varying widely. Existing methods [13, 14, 29, 42, 44], while automating the process, often learn fixed styles and require large datasets and retraining to adapt to new users, which limits their practical application. To address this, image retouching approaches need to be able to adapt to user preferences using only a few reference examples, enabling personalized retouching at test time without the need for extensive retraining or large datasets.

[†]Corresponding authors.

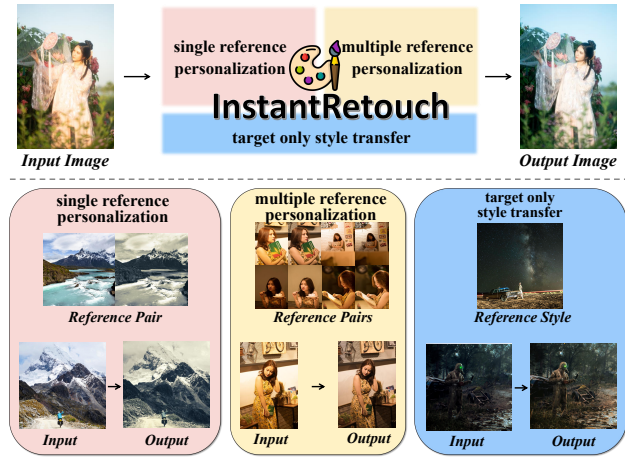


Figure 1. Our proposed method effectively personalizes image retouching from single or multiple references of similar or diverse styles at inference time, with no test-time finetuning. It also supports photorealistic style transfer out of the box.

Several works have explored generic personalized image retouching by conditioning on user-provided reference images [20, 22, 34]. While these methods show promise, their effectiveness is limited by their weak representation of users' retouching styles. Existing techniques such as style classification [34], metric learning [20], and auto-encoding (with architectures not specifically designed to disentangle the retouching style from content) [22] struggle to accurately capture the retouching style, disentangled from the content, that can be effectively applied to a new image. Additionally, they lack the ability to integrate information from multiple reference images, which prevents coherent retouching style fusion from multiple user references and constrains their ability to handle multi-style image retouching personalization.

To overcome these limitations, we introduce **InstantRetouch**, a generic personalized image retouching framework that accurately captures a user's retouching style from a

small set of reference examples and adaptively applies it to new images based on their visual content. Central to our approach is a novel architecture, an *Asymmetric Auto-Encoder*, which encodes the retouching style between an original image and its retouched version into a high-level latent representation. The architecture comprises a twin encoder network with shared weights, a siamese network design, that processes the input and its corresponding retouched target, capturing the color and tone transformations while abstracting away the semantic content. This resulting latent representation is then used as a condition to control a lightweight decoder, implemented as a conditional multi-layer perceptron (MLP) operating in color domain, which faithfully reconstructs the retouched image from the original input. By disentangling retouching style from image semantics, our model enables precise and consistent transfer of the retouching style to a new input image without any fine-tuning at test-time.

Having encoded the retouching style of a pair of images into disentangled latent representations, we introduce *Retrieval-Augmented Retouching (RAR)* to personalize and adaptively retouch new images using style information derived from a user’s preference examples. RAR performs content-aware retouching by retrieving the top- K most relevant reference pairs from the user’s preference set based on visual similarity to the new input image. The corresponding retouching latent codes of these retrieved examples are then aggregated via a weighted average, producing a composite retouch style that reflects the most relevant color and tone transformations for the current input. This aggregated retouching latent, along with the input image, is then passed to the conditional MLP decoder to obtain the final retouched output. Through this retrieval-based conditioning, our method adapts the retouching style not only to the user’s overall preferences but also to the content and context of each input image.

As a result, **InstantRetouch** outperforms existing generic image retouching methods across diverse scenarios, including single or multiple reference examples with the same or varying styles, Figure 1. Although designed for personalized retouching using paired reference images, it also generalizes to photorealistic style transfer with an unpaired single reference image [15, 19, 43], without any retraining, by simply reusing the new input image as a pseudo reference input. This demonstrates the model’s ability to encode retouching styles even from semantically different images. In summary, our contributions include,

- A generic framework for personalized image retouching to instantly adapt user’s retouching style from few reference examples.
- An Asymmetric Auto-Encoder that encodes user preferences into a content-disentangled retouching style latent representation.

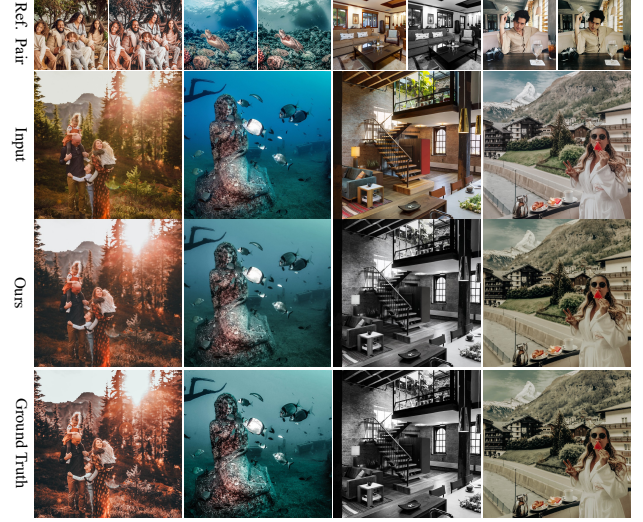


Figure 2. Image retouching style transfer from a single reference pair. *Top*: input–output reference pair defining the retouching style. *Second row*: query input images. *Third row*: our method’s results. *Bottom*: ground-truth retouched images.

- A Retrieval-Augmented Retouching (RAR) module that enables content-adaptive image retouching personalization by combining relevant reference styles.

2. Related works

Image retouching Various methods have been proposed to automate image retouching, from traditional enhancement techniques [13, 28, 42, 44] to learning-based approaches using convolutional networks [7, 14, 18, 38, 40]. However, most of these methods apply a fixed retouching style at test time, limiting their adaptability to diverse user preferences. White-box methods [17, 29, 33] improve user control by allowing manual adjustments, but still require a fixed expert style and user engagement. Methods such as [12, 36, 41] fine-tune models for a few styles, but require retraining for each new user, which limits their practicality. In contrast, our approach enables test-time adaptation to user preferences using a small set of reference examples, without retraining.

Generic personalized retouching Several methods [10, 21, 37] train on diverse styles to produce multiple outputs at inference but do not support personalization via user-provided references. Recent approaches use multi-modal large language models for text-guided retouching [5, 11, 27], but textual descriptions are often too vague to capture a user’s specific retouching intent. Methods like StarEnhancer [34], MSM [22], and PieNet [20] offer test-time personalization with a small set of user-preferred examples but struggle with weak representations and ineffective adaptation to varying image content. Photorealistic

style transfer [15, 19, 24, 43] can perform single-reference color transfer but cannot handle multi-reference personalization or content-aware adaptability. Generic image editing frameworks [2, 3, 6, 25, 32, 39] use visual in-context learning to unify various tasks but perform poorly compared to models specialized for image retouching.

3. Method

3.1. Asymmetric Auto-Encoder

In generic personalized image retouching, the first step is to effectively represent a user’s retouching style from the reference example pairs. StarEnhancer [34] learns a style representation by training a classifier on a fixed set of retouching styles, but this closed-set formulation limits its ability to generalize to unseen styles. PieNet [20] uses metric learning [16] to map images with similar retouching effects close in embedding space. However, the contrastive signal used in this setup is too coarse to capture the fine-grained color and lighting variation that characterizes individual user’s retouching preferences. MSM [22] adopts a U-Net with a conditional decoder to predict the residual between input and retouched images via reconstruction loss, but the resulting representation entangles style with content, preventing robust retouching style transfer to new images with different visual compositions.

To address these limitations, we propose an **asymmetric auto-encoder** that encodes retouching style into a content-disentangled latent representation, enabling faithful reconstruction of the retouched image from its original input. As illustrated in Figure 3, our model comprises a style encoder E_θ , which extracts the retouching style from input-output image pairs, and a lightweight decoder D_ϕ , which reconstructs the retouched image conditioned on the original input and the inferred retouching style representation. Given an original image $x \in \mathcal{X}$ and its user-retouched version $y \in \mathcal{Y}$, the encoder computes a latent vector $z = E_\theta(x, y)$, which captures high-level retouching attributes such as color and tone shifts. The decoder then synthesizes the retouched output as $\hat{y} = D_\phi(x, z)$.

The encoder is implemented as a Siamese network based on the SigLIP-v2 backbone [35], processing both the original and retouched images. Features pooled from both branches are concatenated and passed through a projection layer to form the final retouching style representation $z \in \mathbb{R}^d$. To effectively adapt the encoder to retouching tasks, we add trainable LoRA weights, enabling efficient fine-tuning for retouching style representation learning.

The decoder is designed as a lightweight conditional MLP that operates in color space, mapping per-pixel values from $\mathbb{R}^3 \rightarrow \mathbb{R}^3$. This design is motivated by two key factors. First, it encourages the decoder to rely on the retouching latent z rather than the model parameters during recon-

struction, forcing the latent representation to encode color and lighting transformations that are disentangled from image content; since the differences between input and retouched images is a variation in color and lighting. Second, prior works [9, 14, 42, 44] have demonstrated that operating in color space yields higher image fidelity compared to spatial-domain operators, while also being resolution-agnostic and computationally efficient.

The architecture of the conditional MLP decoder is shown in the top-right of Figure 3. It consists of an input layer followed by N conditional MLP blocks, inspired by feature conditioning in modern transformer [30]. To incorporate the retouching style latent, we project z and add it to the hidden features of each MLP block. While we also experimented with more complex conditioning strategies such as adaptive layer normalization and cross-attention, the simple additive method performed best in our setting, offering a good balance between simplicity and effectiveness.

To train the encoder-decoder pair, we minimize an ℓ_1 reconstruction loss between the predicted and ground truth retouched images:

$$\mathcal{L}_{\text{recon}} = \mathbb{E}_{(x, y) \sim \mathcal{D}} [\|D_\phi(x, E_\theta(x, y)) - y\|_1], \quad (1)$$

where \mathcal{D} is a paired image retouching dataset. This objective encourages the encoder to encode retouch-specific transformations, while the decoder learns to apply these transformations faithfully to the original image. Once trained, our method can now encode the user’s preference pairs, $\mathcal{P} = \{(x_i, y_i)\}_{i=1}^K$ into a retouching style latents, precisely capturing the user’s preferences.

3.2. Retrieval Augmented Retouching

After encoding a user’s preferences into retouching style latents, the next step is applying them to a new query image. StarEnhancer [34] and PieNet [20] average per-pair style embeddings to create a single user preference vector, conditioning retouching on this global code. However, this ignores the content-dependent nature of retouching, as users apply different styles to images based on their content (e.g., overexposed vs. underexposed scenes). MSM [22] models content dependence with a transformer that predicts query style from reference content/style embeddings and the query’s content embedding, trained via meta-learning. However, its meta-learning framework is built on unpaired user images and synthetically degraded pseudo-inputs with limited diversity in color and lighting distributions. Because the inputs are relatively homogeneous while only the outputs vary, the model learns a narrow mapping space focused on reproducing output appearances. Consequently, it struggles to generalize when faced with more complex scenarios where both the input conditions and the desired retouching transformations are diverse.

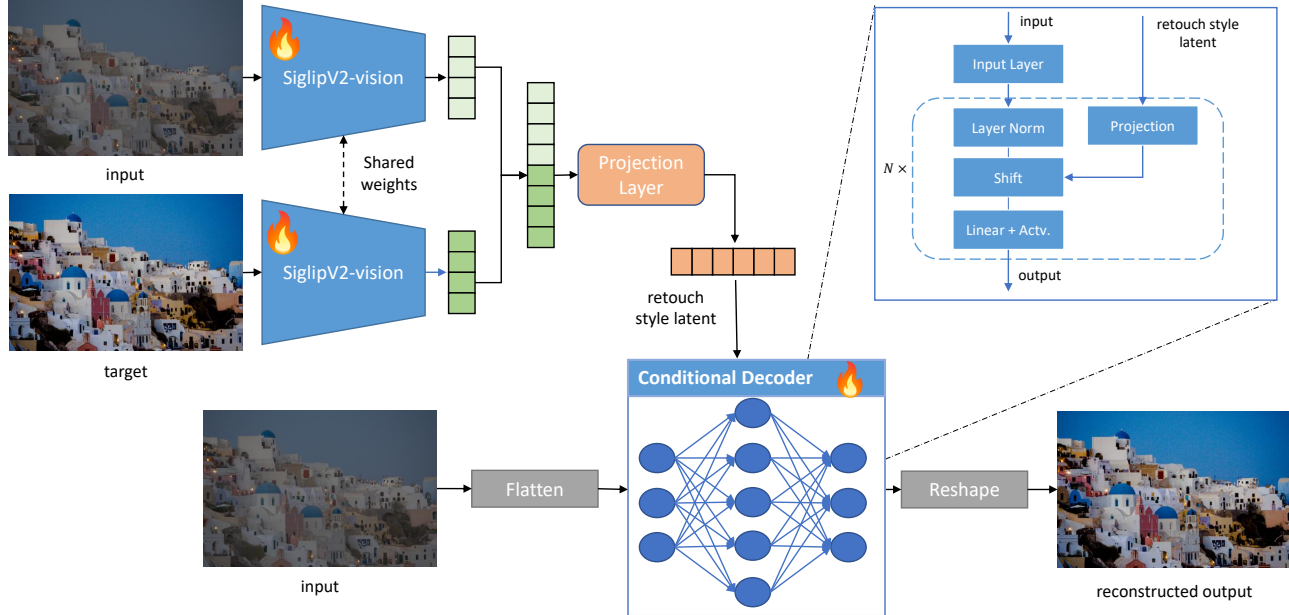


Figure 3. **Illustration of our Asymmetric Auto-encoder.** The asymmetric auto-encoder is the core component of our approach, comprising a LoRA-adapted Siamese encoder and a lightweight conditional MLP decoder. The encoder processes input-output pairs to learn a content-disentangled retouching style representation, encoding it into a compact latent vector. The conditional MLP decoder then applies this latent representation to reconstruct the retouched image from the original input, operating in color space to preserve content while applying the desired retouching style.

In contrast, we propose **retrieval-augmented retouching (RAR)**, to retouch an image based on references relevant to the new image. Given a query image x_q , we first compute its content embedding c_q with a pretrained content encoder (SigLIP-v2). For each reference pair (x_i, y_i) with style latent z_i and content embedding c_i , we measure similarity via cosine similarity $s_i = \frac{c_q \cdot c_i}{\|c_q\| \|c_i\|}$. We then retrieve the top- K nearest neighbors \mathcal{N}_K and aggregate their style latents with a softmax weighting:

$$w_i = \frac{\exp(\frac{s_i}{\tau})}{\sum_{j \in \mathcal{N}_K} \exp(\frac{s_j}{\tau})}, \quad z_q = \sum_{i \in \mathcal{N}_K} w_i z_i, \quad (2)$$

where $\tau > 0$ is the temperature controlling the sharpness of the weighting. The personalized retouching result is then obtained by the conditional decoder as,

$$\hat{y}_q = D_\phi(x_q, z_q). \quad (3)$$

Applying the aggregated style z_q to the query image. By retrieving and weighting styles based on content similarity, RAR adapts user preferences to each image's characteristics rather than enforcing a single global style for every input image.

4. Experiments

4.1. Dataset

To train the asymmetric autoencoder in our **InstantRetouch**, we collect 800 free presets from the Adobe Lightroom community [1] and apply them to 95,000 images sampled from the LAION dataset [31]. This process provides a diverse set of real-world retouching transformations while maintaining a clear separation between training and evaluation domains. To guarantee fair benchmarking, we exclude all benchmark images and transformation types from the training set, in contrast to previous methods that incorporated benchmark content or styles during training [20, 34]. Additional details on the dataset construction, filtering, and preset selection are provided in the supplementary material.

4.2. Experimental set-up

We use SigLIP-v2¹ as the backbone of the Siamese style encoder and add LoRA adapters (rank 16) to all linear layers in the attention blocks. The projection layer takes the concatenation of the features pooled from the two branches and output a 2048-dimensional retouching latent. The conditional MLP decoder operates per pixel in color space, an input layer maps an RGB pixel to a 128-D hidden state, followed by three conditional MLP blocks with hidden di-

¹we particularly use the *google/siglip2-so400m-patch14-384* model as the backbone.

mensions [256, 512, 3], as shown in Figure 3. All intermediate layers use ReLU activations, while the final layer uses a sigmoid to constrain outputs to $[0, 1]$. The retouching latent is injected into the all hidden layers of the MLP decoder after projecting it using a Linear+ReLU to match the target layer’s hidden dimension. This model is then trained for 180,000 steps with a batch size of 8 on (384, 384) random crops of the training images. For content embeddings in Retrieval-Augmented Retouching (RAR), we reuse the pre-trained SigLIP-v2 backbone by disabling LoRA weights. Then, we compute cosine similarity between the query and references’ input embeddings to retrieve the most relevant references using Equation (2). Unless stated otherwise, we set the softmax temperature to $\tau = 0.1$, and $K = 3$ in all the experiments.

4.3. Benchmarks

We evaluate image retouching personalization across three increasingly challenging settings: (1) single-style retouching, (2) multi-style retouching with consistent edits, and (3) multi-style retouching with inconsistent, implicitly defined edits.

VCIRB (Single-Style Retouching): To evaluate personalization under a single, consistent retouching style, we construct the Visually Consistent Image Retouching Benchmark (VCIRB) by applying 25 unseen Adobe Lightroom presets to images sampled from LAION [31]. Since a preset may produce inconsistent results across diverse content [12, 19], we cluster images into 25 semantically and color-tone coherent groups using SigLIP embeddings and *ab*-channel histograms in CIELAB space. Presets are applied within these clusters to ensure visual consistency in the retouched outputs. We compare against several generic personalized image retouching baselines: StarEnhancer [34], MSM [22], VisualCloze [25] (a generic in-context generative editing model), PhotoArtAgent [5], Seedream4.0 [32] and NanoBanana [2]. PhotoArtAgent, Seedream 4.0, and NanoBanana are evaluated only on single-pair personalization, as they are constrained by a short effective context window, where using more than two images as input leads to degraded performance. We also include retrained variants of MSM and VisualCloze, trained on our meta-learning dataset in which 800 Lightroom presets are applied to 95,000 LAION images clustered by semantic content and tonal similarity, following the same protocol as VCIRB (see supplementary material for dataset construction details).

PPR10K-Groups (Multi-Style, Consistent Retouching): In real-world scenarios such as event or portrait photography, users often retouch related images into a consistent output style. The PPR10K dataset [26] groups portrait images of the same subjects captured in different scenes, along with their expert-retouched versions, where experts are instructed to apply consistent adjustments across all images

within a group. This inherent style consistency allows a few reference samples from a group to effectively capture the user’s retouching preferences, while the variation in scene content provides a natural testbed for evaluating a model’s context-awareness. We select 21 PPR10K groups, retouched by expert A, with more than 12 images each and sample 1, 3, or 6 reference pairs per group and test on the remaining images. We compare with the same baselines as in VCIRB, testing each model’s ability to handle multiple references in a multi-style setting.

MIT-FiveK and PPR10K Users (Multi-Style, Inconsistent Retouching): Another common use case is adapting to a user’s retouching style from historical edits, which is often diverse and inconsistent. This setting is widely used in prior personalization works [22, 29, 42]. We follow the standard protocol on MIT-Adobe FiveK [4] and PPR10K [26] to split the datasets into training and test splits. From each training split, we sample 20, 50, and 100 input–output reference pairs and evaluate on the test sets (498 for FiveK and 2,286 for PPR10K). Unlike prior work [22], we explicitly sample references based on color and tone diversity to minimize distribution mismatch between reference and test images. These fixed references are then used for all methods. Further details of the sampling strategy are provided in the supplementary material. To compare our method, we select baselines capable of handling more than 20 references. While VisualCloze can theoretically accommodate any number of references, its computational complexity increases rapidly as the number of references grows, since it directly processes the patchified 2D latent encodings of the reference pairs using a large diffusion transformer. Therefore, we exclude it from comparison in this setting. Additionally, we include two state-of-the-art, training-based image personalization methods: AdaInt [42] and RSFNet [29] to assess and compare their performance when training data is limited. Both are trained on the reference images for 100 epochs using their default configurations. Note that we exclude StarEnhancer from the evaluation on the MIT-FiveK data because the model has already been trained on MIT-FiveK.

All images in VCIRB are resized to 512x512, while the original resolution is maintained for images from MIT-FiveK and PPR10K. For VisualCloze, we pre-resize the images to be divisible by 16 using a right crop, and evaluate them at this resolution to prevent loss due to VAE downampling and patchification. PSNR, SSIM, and LPIPS are used to evaluate image retouching personalization performance across all three benchmarks. The reported metrics are averaged over all test images and across groups (if applicable).

4.4. Results

Reconstruction As shown in Table 1, we compare the reconstruction fidelity of InstantRetouch with MSM [22], an

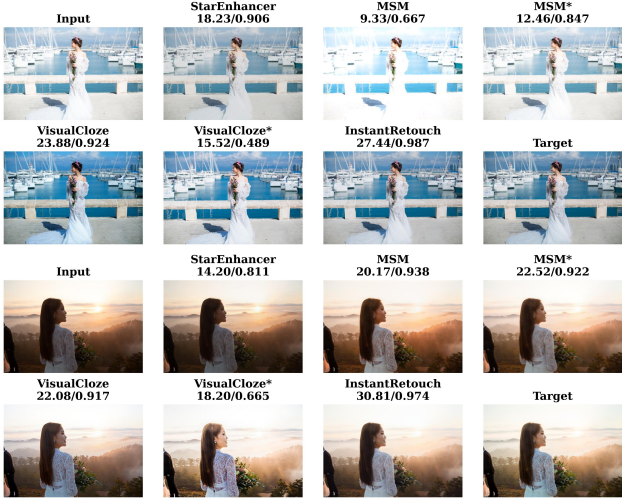


Figure 4. PPR10K groups performance comparison when three references are used.

Table 1. Reconstruction fidelity comparison. \dagger indicates that the baseline model is trained on our dataset.

Dataset	Method	PSNR↑	SSIM↑	LPIPS↓
VCIRB	MSM [22]	27.28	0.900	0.099
	MSM \dagger [22]	29.61	0.923	0.069
	Ours	32.42	0.974	0.035
MIT-Fivek	MSM [22]	28.94	0.851	0.137
	MSM \dagger [22]	26.32	0.803	0.199
	Ours	32.95	0.972	0.028
PPR10K-A	MSM [22]	29.28	0.943	0.075
	MSM \dagger [22]	29.71	0.936	0.086
	Ours	34.14	0.984	0.019

approach that learns a retouching latent through a reconstruction objective. We evaluate both the original MSM checkpoint and another version trained on the same dataset as ours for a fair comparison. Across the VCIRB benchmark and paired examples from MIT-Adobe FiveK [4] and PPR10K [26], InstantRetouch consistently outperforms both MSM variants. These results demonstrate that our model (i) encodes retouching styles effectively into a low-dimensional latent vector and (ii) faithfully reconstructs the retouched output from the original image and the learned latent representation.

Personalization of a single retouching Reconstruction alone is not sufficient; the learned retouching latent must be disentangled from image content to enable style transfer to new query images, a key requirement for personalized retouching. To evaluate this, we extract the retouching latent from a single reference pair and apply it to unseen query images. As shown in Figure 2, InstantRetouch accu-

rately transfers the retouching style from the reference to the query images using only the latent representation. These results indicate that the encoded latent representation is effectively disentangled from image content, enabling it to capture the retouching style in the reference pair while remaining invariant to scene semantics. Quantitative results on the VCIRB benchmark in Table 2 further support this finding; our method significantly outperforms existing generic retouching transfer approaches. For evaluations with multiple reference pairs, we use Retrieval-Augmented Retouching (RAR) to aggregate style cues from relevant references. However, increasing the number of references results in only marginal improvements on VCIRB, which is expected since all images in a given VCIRB group are retouched with the same preset, making a single reference sufficient to capture the style.

Personalization of multiple consistent retouching styles

Table 2 also provides the performance on the PPR10K-groups dataset, and similarly our method consistently outperforms existing generic retouching personalization approaches. Notably, performance improves as more reference examples are added, in contrast to the high inconsistency seen in other methods. This highlights the effectiveness of our Retrieval-Augmented Retouching(RAR) in leveraging multiple references for content-aware retouching, adapting the style based on the input image’s context. Qualitative comparisons using three reference examples are presented in Figure 4.

Personalization with multiple and inconsistent retouching styles The results in Table 4 show the performance of personalizing to MIT-FiveK and PPR10K users’ retouching style. Our approach surpasses all generic personalized retouching baselines and achieves performance comparable to, or even exceeding, methods explicitly trained on the specific individual user references [29, 42], despite being entirely tuning free. This highlights the strong personalization capability of our approach and its ability to generalize to challenging image retouching personalization scenarios. Consistent with the PPR10K-groups evaluation, performance improves with additional reference images, highlighting the model’s ability to leverage multiple example, especially in cases involving diverse retouching styles.

Photorealistic Style Transfer. Our method naturally supports photorealistic style transfer, in which the color and tonal characteristics of an unpaired style reference are applied to a content image while preserving its structure and semantics [citeho2021deep](#), [ke2023neural](#), [yoo2019photorealistic](#). This is achieved by forming a pseudo reference pair, re-using the content image as the input and the style image as the target, and then applying our standard pipeline without any task-specific tuning. The visual results in Figure 5 and the quantitative results in Table 3, evaluated using metrics from [19], demonstrate that

Table 2. Image retouching personalization comparison on the VCIRB and PPR10K groups benchmarks. The best results are shown in bold. \dagger indicates methods that are re-trained (or fine-tuned) on our dataset.

Dataset	Method	PSNR \uparrow			SSIM \uparrow			LPIPS \downarrow		
		1	2	4	1	2	4	1	2	4
VCIRB	StarEnhancer [34]	21.00	20.98	21.27	0.864	0.863	0.868	0.123	0.123	0.120
	MSM [22]	17.69	18.17	18.53	0.822	0.830	0.836	0.164	0.155	0.150
	MSM \dagger [22]	24.35	25.03	25.28	0.900	0.904	0.905	0.097	0.094	0.093
	VisualCloze [25]	19.81	18.60	12.05	0.765	0.731	0.378	0.173	0.191	0.591
	VisualCloze \dagger [25]	23.91	24.63	24.70	0.83	0.834	0.825	0.077	0.072	0.079
	PhotoArtAgent [5]	20.03	-	-	0.83	-	-	0.158	-	-
	NanoBanana [2]	11.61	-	-	0.387	-	-	0.570	-	-
	Seedream4.0 [32]	11.8	-	-	0.422	-	-	0.488	-	-
	Ours	29.13	29.57	29.82	0.963	0.964	0.965	0.048	0.047	0.046
PPR10K-groups		1	3	6	1	3	6	1	3	6
	StarEnhancer [34]	19.16	18.83	19.36	0.875	0.857	0.866	0.102	0.108	0.119
	MSM [22]	18.86	18.82	18.59	0.877	0.873	0.878	0.154	0.159	0.155
	MSM \dagger [22]	19.27	19.62	18.16	0.876	0.880	0.866	0.149	0.148	0.170
	VisualCloze [25]	15.04	14.21	7.74	0.453	0.432	0.246	0.22	0.261	0.844
	VisualCloze \dagger [25]	21.12	21.42	20.98	0.832	0.832	0.812	0.097	0.093	0.112
	PhotoArtAgent [5]	20.01	-	-	0.888	-	-	0.093	-	-
	NanoBanana [2]	12.89	-	-	0.48	-	-	0.434	-	-
	Seedream4.0 [32]	9.34	-	-	0.278	-	-	0.607	-	-
	Ours	22.51	23.92	25.27	0.932	0.949	0.961	0.065	0.052	0.043

Table 3. Photorealistic style transfer quantitative results. Metrics follow [19]. Higher Content and Style Scores indicate better structure preservation and style fidelity, respectively.

Method	Content Score \uparrow	Style Score \uparrow
NeuralPreset [19]	0.856	0.555
DeepPreset [15]	0.913	0.616
D-LUT [23]	0.787	0.657
PhotoArtAgent [5]	0.860	0.530
PhotoWCT2 [8]	0.749	0.916
NanoBanana [2]	0.658	0.610
Seedream 4.0 [32]	0.454	0.461
Ours	0.742	0.917

our method achieves superior style transfer performance while faithfully preserving content compared to state-of-the-art Photorealistic style transfer methods [8, 15, 19, 23] as well as generic image editing models [2, 32]. This indicates the ability of our model to encode retouching style between two semantically different images. The evaluations are conducted on the VCIRB benchmark, where the target image of each reference pair, in the single-reference setup, is used as the style exemplar.

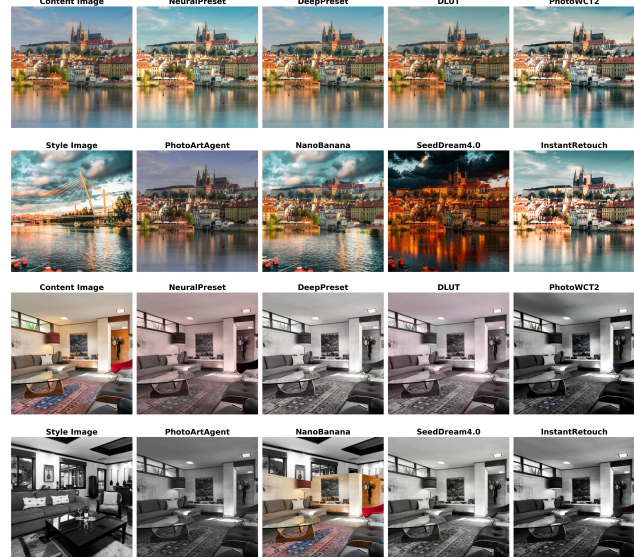


Figure 5. Photorealistic style transfer comparison. Our method can be used for photorealistic style transfer, applying color and tone from a single unpaired reference out of the box.

4.5. Ablation Study

To validate the architectural design and evaluate the contribution of individual components in the asymmetric auto-

Table 4. Image personalization with few reference samples on the standard MIT-FiveK and PPR10K benchmark datasets. While MSM, StarEnhancer, and our method don't require user-specific training, AdaInt and RSFNet require training on individual user's reference samples.

Dataset	Method	PSNR↑			SSIM↑			LPIPS↓		
		20	50	100	20	50	100	20	50	100
MIT-Fivek [4]	MSM [22]	22.13	21.79	22.05	0.807	0.806	0.807	0.171	0.174	0.171
	MSM [†] [22]	20.46	20.48	20.58	0.750	0.753	0.753	0.238	0.236	0.234
	AdaInt [42]	20.12	20.80	22.49	0.824	0.833	0.854	0.111	0.098	0.078
	RSFNet [10]	22.52	22.87	22.66	0.862	0.866	0.86	0.072	0.069	0.072
	Ours	22.95	23.19	23.34	0.913	0.917	0.920	0.070	0.067	0.067
PPR10K [26]	StarEnhancer [34]	20.54	20.57	20.64	0.880	0.878	0.882	0.085	0.086	0.085
	MSM [22]	19.48	19.98	20.06	0.866	0.873	0.873	0.146	0.138	0.134
	MSM [†] [22]	20.94	21.21	21.38	0.871	0.875	0.878	0.117	0.117	0.116
	AdaInt [42]	21.28	22.08	22.82	0.903	0.921	0.932	0.077	0.065	0.058
	RSFNet [29]	22.01	22.08	22.22	0.923	0.924	0.923	0.069	0.067	0.065
	Ours	21.75	22.30	22.47	0.935	0.941	0.942	0.070	0.065	0.063

Table 5. Ablation study for the **asymmetric auto-encoder** in InstantRetouch. We compare three encoder backbones: *RN-50* (ResNet-50), *SL-F* (frozen SigLIP), and *SL-LoRA* (SigLIP with LoRA adapters). Decoder variants include our proposed conditional *MLP* and the *UNET*-based decoder from [22]. We also evaluate three conditioning strategies: additive (*Add*), adaptive layer normalization (*AdaIN*), and cross-attention (*Cross-attn*).

Exp №	Encoder			Decoder		Cond-Method			Metrics	
	RN-50	SL-F	SL-LoRA	MLP	UNET	Add	AdaIN	Cross-attn	PSNR↑	SSIM↑
1	×	×	✓	✓	×	✓	×	×	32.40	0.977
2	✓	×	×	✓	×	✓	×	×	30.00	0.971
3	×	✓	×	✓	×	✓	×	×	23.41	0.931
4	×	×	✓	×	✓	×	×	×	29.58	0.944
5	×	×	✓	✓	×	×	✓	×	31.93	0.977
6	×	×	✓	✓	×	×	×	✓	22.66	0.880

encoder of *InstantRetouch*, we conduct a comprehensive ablation study by varying the encoder backbone, decoder architecture, and conditioning method, as summarized in Table 5. All models are trained for 10,000 iterations on a subset of the training data with a batch size of 8. Reconstruction fidelity is evaluated on a held-out validation set using PSNR and SSIM metrics. In experiments 1–3, we observe that using a SigLIP-v2 encoder with trainable LoRA adapters significantly outperforms both the ResNet-50 and frozen SigLIP variants. This highlights that strong pretrained features alone are insufficient; adaptation to the retouching task is essential for meaningful style extraction. Additionally, comparing experiments 1 and 4 shows that our proposed lightweight MLP decoder operating in color space yields better reconstruction performance than the UNET-based decoder, supporting the effectiveness of our asymmetric design. This validates our hypothesis that a simpler, per-pixel decoder encourages the encoder to learn a compact and content-disentangled retouching style latent. Ex-

periments 5 and 6 further demonstrate that simple additive conditioning injection outperforms adaptive layer norm and cross-attention alternatives. For conditioning the UNET decoder with the retouching latent, we adopt the approach in [22]. Moreover, we ablated the loss function by adding auxiliary terms such as KL divergence, GAN, and LPIPS losses, but these resulted in lower PSNR scores of 20.84, 30.64, and 31.66, respectively, underperforming the simple L1 loss.

Table 6 shows the image personalization performance on MIT-FiveK, varying the number of relevant references used to compute the retouching style, as in Equation (2). Performance improves with more relevant references, demonstrating the model's ability to utilize multiple inputs. However, using all the references results in poor performance, highlighting the importance of selecting relevant samples and emphasizing the effectiveness of our retrieval-augmented retouching approach.

Table 6. Image personalization performance with varying top_K , number of relevant references.

Ref #	k=1	k=3	k=5	All
20	21.44/0.889	22.95/0.913	23.37/0.918	21.99/0.897
50	21.47/0.899	23.19/0.917	23.56/0.920	21.97/0.898
100	21.94/0.900	23.34/0.920	23.82/0.923	21.94/0.897

Acknowledgements

This work was supported by the Zhejiang Provincial Natural Science Foundation of China under Grant No. LD24F020007.

5. Conclusion

We proposed a generic personalized image retouching framework that adapts to individual user’s style from only a handful of reference pairs without test-time finetuning. Experiments across three benchmarks of increasing complexity show that our proposed method consistently outperforms existing generic image retouching personalization methods. In addition, the same pipeline can be used out of the box for photorealistic style transfer, highlighting its versatility and generalization across tasks.

References

- [1] Adobe Inc. Adobe lightroom community presets, 2025. Accessed 2025-05-11. [4](#), [12](#)
- [2] Google AI. Image generation with gemini (aka nano banana). <https://ai.google.dev/gemini-api/docs/image-generation>, 2025. Accessed: 2025-11-12. [3](#), [5](#), [7](#)
- [3] Amir Bar, Yossi Gandelsman, Trevor Darrell, Amir Globerson, and Alexei Efros. Visual prompting via image inpainting. *Advances in Neural Information Processing Systems*, 35:25005–25017, 2022. [3](#)
- [4] Vladimir Bychkovsky, Sylvain Paris, Eric Chan, and Frédéric Durand. Learning photographic global tonal adjustment with a database of input / output image pairs. In *The Twenty-Fourth IEEE Conference on Computer Vision and Pattern Recognition*, 2011. [5](#), [6](#), [8](#), [12](#)
- [5] Haoyu Chen, Keda Tao, Yizao Wang, Xinlei Wang, Lei Zhu, and Jinjin Gu. Photoartagent: Intelligent photo retouching with language model-based artist agents. *arXiv preprint arXiv:2505.23130*, 2025. [2](#), [5](#), [7](#)
- [6] Lan Chen, Qi Mao, Yuchao Gu, and Mike Zheng Shou. Edit transfer: Learning image editing via vision in-context relations. *arXiv preprint arXiv:2503.13327*, 2025. [3](#)
- [7] Yu-Sheng Chen, Yu-Ching Wang, Man-Hsin Kao, and Yung-Yu Chuang. Deep photo enhancer: Unpaired learning for image enhancement from photographs with gans. In *Proceedings of the IEEE conference on computer vision and pattern recognition*, pages 6306–6314, 2018. [2](#)
- [8] Tai-Yin Chiu and Danna Gurari. Photowct2: Compact autoencoder for photorealistic style transfer resulting from blockwise training and skip connections of high-frequency residuals. In *Proceedings of the IEEE/CVF winter conference on applications of computer vision*, pages 2868–2877, 2022. [7](#)
- [9] Marcos V Conde, Javier Vazquez-Corral, Michael S Brown, and Radu Timofte. Nilut: Conditional neural implicit 3d lookup tables for image enhancement. In *Proceedings of the AAAI Conference on Artificial Intelligence*, 2024. [3](#)
- [10] Zheng-Peng Duan, Jiawei Zhang, Zheng Lin, Xin Jin, Xun-Dong Wang, Dongqing Zou, Chun-Le Guo, and Chongyi Li. Diffretouch: Using diffusion to retouch on the shoulder of experts. In *Proceedings of the AAAI Conference on Artificial Intelligence*, 2025. [2](#), [8](#)
- [11] Niladri Shekhar Dutt, Duygu Ceylan, and Niloy J Mitra. Monetgpt: Solving puzzles enhances mllms’ image retouching skills. *arXiv preprint arXiv:2505.06176*, 2025. [2](#)
- [12] Omar Elezabi, Marcos V Conde, Zongwei Wu, and Radu Timofte. Inretouch: Context aware implicit neural representation for photography retouching. *arXiv preprint arXiv:2412.03848*, 2024. [2](#), [5](#), [12](#)
- [13] Michaël Gharbi, Jiawen Chen, Jonathan T Barron, Samuel W Hasinoff, and Frédéric Durand. Deep bilateral learning for real-time image enhancement. *ACM Transactions on Graphics (TOG)*, 36(4):1–12, 2017. [1](#), [2](#)
- [14] Jingwen He, Yihao Liu, Yu Qiao, and Chao Dong. Conditional sequential modulation for efficient global image retouching. In *Computer Vision–ECCV 2020: 16th European Conference, Glasgow, UK, August 23–28, 2020, Proceedings, Part XIII 16*, pages 679–695. Springer, 2020. [1](#), [2](#), [3](#)
- [15] Man M Ho and Jinjia Zhou. Deep preset: Blending and retouching photos with color style transfer. In *Proceedings of the IEEE/CVF Winter Conference on Applications of Computer Vision*, pages 2113–2121, 2021. [2](#), [3](#), [7](#), [12](#)
- [16] Elad Hoffer and Nir Ailon. Deep metric learning using triplet network. In *International workshop on similarity-based pattern recognition*, pages 84–92. Springer, 2015. [3](#)
- [17] Yuanming Hu, Hao He, Chenxi Xu, Baoyuan Wang, and Stephen Lin. Exposure: A white-box photo post-processing framework. *ACM Transactions on Graphics (TOG)*, 37(2):1–17, 2018. [2](#)
- [18] Phillip Isola, Jun-Yan Zhu, Tinghui Zhou, and Alexei A Efros. Image-to-image translation with conditional adversarial networks. In *Proceedings of the IEEE conference on computer vision and pattern recognition*, pages 1125–1134, 2017. [2](#)
- [19] Zhanghan Ke, Yuhao Liu, Lei Zhu, Nanxuan Zhao, and Rynson WH Lau. Neural preset for color style transfer. In *Proceedings of the IEEE/CVF conference on computer vision and pattern recognition*, pages 14173–14182, 2023. [2](#), [3](#), [5](#), [6](#), [7](#), [12](#)
- [20] Han-Ul Kim, Young Jun Koh, and Chang-Su Kim. Pienet: Personalized image enhancement network. In *Computer Vision–ECCV 2020: 16th European Conference, Glasgow, UK, August 23–28, 2020, Proceedings, Part XXX 16*, pages 374–390. Springer, 2020. [1](#), [2](#), [3](#), [4](#)

[21] Jiwon Kim, Soohyun Hwang, Dong-O Kim, Changsu Han, Min Kyu Park, and Chang-Su Kim. Oneta: Multi-style image enhancement using eigentransformation functions. *arXiv preprint arXiv:2506.23547*, 2025. 2

[22] Satoshi Kosugi and Toshihiko Yamasaki. Personalized image enhancement featuring masked style modeling. *IEEE Transactions on Circuits and Systems for Video Technology*, 34(1):140–152, 2024. 1, 2, 3, 5, 6, 7, 8, 12

[23] Mujing Li, Guanjie Wang, Xingguang Zhang, Qifeng Liao, and Chenxi Xiao. D-lut: Photorealistic style transfer via diffusion process. In *2025 IEEE/CVF Winter Conference on Applications of Computer Vision (WACV)*, pages 9206–9214. IEEE, 2025. 7

[24] Yijun Li, Ming-Yu Liu, Xuetong Li, Ming-Hsuan Yang, and Jan Kautz. A closed-form solution to photorealistic image stylization. In *Proceedings of the European conference on computer vision (ECCV)*, pages 453–468, 2018. 3

[25] Zhong-Yu Li, Ruoyi Du, Juncheng Yan, Le Zhuo, Zhen Li, Peng Gao, Zhanyu Ma, and Ming-Ming Cheng. Visual-cloze: A universal image generation framework via visual in-context learning. *arXiv preprint arXiv:2504.07960*, 2025. 3, 5, 7

[26] Jie Liang, Hui Zeng, Miaomiao Cui, Xuansong Xie, and Lei Zhang. Ppr10k: A large-scale portrait photo retouching dataset with human-region mask and group-level consistency. In *Proceedings of the IEEE/CVF Conference on Computer Vision and Pattern Recognition*, pages 653–661, 2021. 5, 6, 8, 12, 13

[27] Yunlong Lin, Zixu Lin, Kunjie Lin, Jinbin Bai, Panwang Pan, Chenxin Li, Haoyu Chen, Zhongdao Wang, Xinghao Ding, Wenbo Li, et al. Jarvisart: Liberating human artistic creativity via an intelligent photo retouching agent. *arXiv preprint arXiv:2506.17612*, 2025. 2

[28] Sean Moran, Pierre Marza, Steven McDonagh, Sarah Parisot, and Gregory Slabaugh. Deeplpf: Deep local parametric filters for image enhancement. In *Proceedings of the IEEE/CVF conference on computer vision and pattern recognition*, pages 12826–12835, 2020. 2

[29] Wenqi Ouyang, Yi Dong, Xiaoyang Kang, Peiran Ren, Xin Xu, and Xuansong Xie. Rsfnet: A white-box image retouching approach using region-specific color filters. In *Proceedings of the IEEE/CVF International Conference on Computer Vision*, pages 12160–12169, 2023. 1, 2, 5, 6, 8

[30] William Peebles and Saining Xie. Scalable diffusion models with transformers. In *Proceedings of the IEEE/CVF international conference on computer vision*, pages 4195–4205, 2023. 3

[31] Christoph Schuhmann, Romain Beaumont, Richard Vencu, Cade Gordon, Ross Wightman, Mehdi Cherti, Theo Coombes, Aarush Katta, Clayton Mullis, Mitchell Wortsman, et al. Laion-5b: An open large-scale dataset for training next generation image-text models. *Advances in neural information processing systems*, 35:25278–25294, 2022. 4, 5, 12

[32] Team Seedream, Yunpeng Chen, Yu Gao, Lixue Gong, Meng Guo, Qiushan Guo, Zhiyao Guo, Xiaoxia Hou, Weilin Huang, Yixuan Huang, et al. Seedream 4.0: Toward next-generation multimodal image generation. *arXiv preprint arXiv:2509.20427*, 2025. 3, 5, 7

[33] Jing Shi, Ning Xu, Yihang Xu, Trung Bui, Franck Dernoncourt, and Chenliang Xu. Learning by planning: Language-guided global image editing. In *Proceedings of the IEEE/CVF Conference on Computer Vision and Pattern Recognition*, pages 13590–13599, 2021. 2

[34] Yuda Song, Hui Qian, and Xin Du. Starenhancer: Learning real-time and style-aware image enhancement. In *Proceedings of the IEEE/CVF International Conference on Computer Vision*, pages 4126–4135, 2021. 1, 2, 3, 4, 5, 7, 8, 12

[35] Michael Tschannen, Alexey Gritsenko, Xiao Wang, Muhammad Ferjad Naeem, Ibrahim Alabdulmohsin, Nikhil Parthasarathy, Talfan Evans, Lucas Beyer, Ye Xia, Basil Mustafa, et al. Siglip 2: Multilingual vision-language encoders with improved semantic understanding, localization, and dense features. *arXiv preprint arXiv:2502.14786*, 2025. 3, 12

[36] Ethan Tseng, Yuxuan Zhang, Lars Jebe, Xuaner Zhang, Zhi-hao Xia, Yifei Fan, Felix Heide, and Jiawen Chen. Neural photo-finishing. *ACM Trans. Graph.*, 41(6):238–1, 2022. 2

[37] Haolin Wang, Jiawei Zhang, Ming Liu, Xiaohe Wu, and Wangmeng Zuo. Learning diverse tone styles for image retouching. *IEEE Transactions on Image Processing*, 33:310–321, 2023. 2

[38] Ruixing Wang, Qing Zhang, Chi-Wing Fu, Xiaoyong Shen, Wei-Shi Zheng, and Jiaya Jia. Underexposed photo enhancement using deep illumination estimation. In *Proceedings of the IEEE/CVF conference on computer vision and pattern recognition*, pages 6849–6857, 2019. 2

[39] Xinlong Wang, Wen Wang, Yue Cao, Chunhua Shen, and Tiejun Huang. Images speak in images: A generalist painter for in-context visual learning. In *Proceedings of the IEEE/CVF Conference on Computer Vision and Pattern Recognition*, pages 6830–6839, 2023. 3

[40] Yili Wang, Xin Li, Kun Xu, Dongliang He, Qi Zhang, Fu Li, and Errui Ding. Neural color operators for sequential image retouching. In *European Conference on Computer Vision*, pages 38–55. Springer, 2022. 2

[41] Jiarui Wu, Yujin Wang, Lingen Li, Fan Zhang, and Tianfan Xue. Goal conditioned reinforcement learning for photo finishing tuning. *Advances in Neural Information Processing Systems*, 37:46294–46318, 2024. 2

[42] Canqian Yang, Meiguang Jin, Xu Jia, Yi Xu, and Ying Chen. Adaint: Learning adaptive intervals for 3d lookup tables on real-time image enhancement. In *Proceedings of the IEEE/CVF Conference on Computer Vision and Pattern Recognition*, pages 17522–17531, 2022. 1, 2, 3, 5, 6, 8, 13

[43] Jaejun Yoo, Youngjung Uh, Sanghyuk Chun, Byeongkyu Kang, and Jung-Woo Ha. Photorealistic style transfer via wavelet transforms. In *Proceedings of the IEEE/CVF international conference on computer vision*, pages 9036–9045, 2019. 2, 3

[44] Hui Zeng, Jianrui Cai, Lida Li, Zisheng Cao, and Lei Zhang. Learning image-adaptive 3d lookup tables for high performance photo enhancement in real-time. *IEEE Transactions*

on *Pattern Analysis and Machine Intelligence*, 44(4):2058–2073, 2020. [1](#), [2](#), [3](#)

6. Visually Consistent Image Retouching Dataset

Training a generic few-shot image retouching model [22, 34] requires a large and diverse set of retouching styles for meta-learning. However, existing datasets such as MIT-FiveK [4] and PPR10K [26] include images retouched by only five and three experts, respectively. In addition to this limited stylistic diversity, the human edits in these datasets are often inconsistent across images, making them unsuitable for generic retouching tasks. The method in [22] attempts to expand stylistic variety by collecting human-retouched images from Flickr, but these samples contain only the retouched targets and lack their corresponding original inputs. To overcome this, the authors train a degradation model on the paired MIT-FiveK dataset to approximate pseudo-inputs by mapping the targets back to their presumed originals. Yet, because MIT-FiveK primarily consists of underexposed images, the resulting pseudo-inputs are still limited in diversity and fail to generalize to broader content.

Several works [12, 15, 19] construct large-scale retouching datasets by applying Adobe Lightroom presets [1] to collections of images. While this preset-based strategy increases style diversity, applying presets indiscriminately across random images can lead to visually inconsistent results, since the same preset affects different images differently depending on their context. To address this, we construct a visually consistent retouching dataset by applying carefully curated Lightroom presets to images grouped by coherent semantics and color distributions. To ensure diverse input contexts, we sample high-resolution images from the LAION dataset [31], covering a wide range of colors, tones, and semantic content.

To reduce style variance within each group, we organize the images using a two-stage clustering approach. First, we categorize them into 30 distinct semantic groups using the vision-language embeddings from the pretrained SIGLIP-V2 model [35]. Then, within each semantic category, we apply K-means clustering based on the 2D histogram of the ab channels in the Lab color space, ensuring that images within a sub-cluster share similar color characteristics. We choose the number of clusters to balance granularity, keeping them small enough to maintain color consistency, yet large enough to preserve diversity. This results in a total of **2,373** distinct groups.

Once images are grouped by both semantic content and color distribution, we apply carefully curated Adobe Lightroom presets to each group. We curate a set of 830 Lightroom presets by selecting sRGB images to avoid clipping artifacts and filtering out presets that involve masks, vignetting, geometric transformations (e.g., cropping), or texture enhancements. These types of edits cannot be easily



Figure 6. Effects of applying a single preset to different types of images. The preset produces varying results depending on the input’s context, primarily its semantics and color distribution. Left: Applying the preset to a random set of images leads to inconsistent styles. Right: A style group from our dataset, applying the preset to images with similar context results in perceptually consistent style groups, enabling that enable learning effective few-shot image retouching

transferred across different images to build consistent retouching styles. Therefore, we limit our scope to presets that perform only color and tone transformations.

To avoid contextually mismatched edits that may yield degraded results, we pre-filter presets by matching the semantic labels of the image groups to those of the images they were originally applied to. Through this process, we associate 40 suitable presets with each image group, resulting in a consistent image retouching dataset comprising **94,400** stylized image groups. As illustrated in Figure 6, applying the same preset to a semantically and chromatically coherent group produces perceptually consistent results across all images. This consistency is crucial for meta-learning image retouching, as both reference and query images can be reliably sampled from the same style group. In contrast to datasets where presets are applied to randomly selected images, our approach ensures that reference pairs offer informative and contextually relevant guidance for retouching the query images.

7. Benchmark datasets

We evaluate image retouching personalization across three increasingly challenging settings: (1) single-style retouching, (2) multi-style retouching with consistent edits, and (3) multi-style retouching with inconsistent, implicitly defined edits.

Visually Consistent Image Retouching Benchmark (VCIRB): To evaluate generic image retouching methods’ under consistent retouching set-up where both the reference and test pairs follow the same retouching transformation, we construct the VCIRB benchmark. We hold out 25 groups of images, each edited by a distinct Lightroom preset, from the dataset described in Section 6. Both the images and the corresponding presets are excluded from training to ensure unbiased evaluation of models’ generalization to unseen images and styles. For each held-out group, one or more reference pairs are then samples to be used as exemplar to retouch the remaining images in the group and evaluate the image retouching model’s performance in adapting the retouching style from the given reference pairs and applying them in the test images by comparing the results with the ground truth targets.

PPR10k-Groups: The performance of a model under a consistent retouching setup (as in VCIRB) reflects its capacity to understand and replicate the retouching transformation exemplified in the given reference images. However, in practice, users often seek to contextually retouch images by providing a set of diverse reference examples. For example, in event or portrait photography, users may first retouch a few representative images and then use these as references to batch-retouch a large collection of images captured under similar conditions. In these scenarios, images that share similar input contexts, such as scenery, tone, or color attributes, are expected to exhibit similar retouching style adjustments. To evaluate a model’s performance in such context-aware scenarios, we employ the PPR10K dataset [26]. This dataset groups portrait images of subjects captured across varying scenes, where professional experts have applied consistent retouching styles within each group. This inherent style consistency guarantees that only a few reference samples within a group are sufficient to convey the user’s retouching preferences, while the variation in scene context (e.g., backgrounds, lighting, tones) naturally tests a model’s ability to adapt those preferences to different input conditions. We select 21 PPR10K groups retouched by Expert A, each containing more than 12 images. We select 21 PPR10K groups retouched by Expert A, each containing more than 12 images.

MIT-Fivek and PPR10k: We also evaluated image retouching adaptation using the standard MIT-FiveK and PPR10K datasets, which focus on retouching personalization based on a user’s historical edits and stylistic preferences. These datasets contain images retouched by multiple experts, each forming a distinct user style, and are divided into predefined training and testing splits. The training split is used to learn or adapt to a particular user’s retouching style, while the corresponding test split evaluates the model’s personalization performance on unseen images. Unlike the first two setups, the retouching styles in this con-

Algorithm 1 Diverse and Representative Reference Set Sampling

```

Require: Feature set  $\mathcal{H} = \{\mathbf{h}_1, \mathbf{h}_2, \dots, \mathbf{h}_n\}$ , sample size  $k$ , distance function  $d(\cdot, \cdot)$ 
Ensure: Selected indices  $\mathcal{S} \subset \{1, 2, \dots, n\}$  with  $|\mathcal{S}| = k$ 
1:  $\mathcal{S}_0 \leftarrow \emptyset, \mathcal{C}_0 \leftarrow \{1, 2, \dots, n\}$ 
2: // Initialize with most representative sample
3:  $s_1 \leftarrow \arg \min_{i \in \mathcal{C}_0} \left[ \frac{1}{n-1} \sum_{j \in \mathcal{C}_0 \setminus \{i\}} d(\mathbf{h}_i, \mathbf{h}_j) \right]$ 
4:  $\mathcal{S}_1 \leftarrow \{s_1\}, \mathcal{C}_1 \leftarrow \mathcal{C}_0 \setminus \{s_1\}$ 
5: for  $t = 2$  to  $k$  do
6:   // Compute diversity scores
7:   for  $c \in \mathcal{C}_{t-1}$  do
8:      $\mathcal{D}_{\text{ref}}(c) \leftarrow \frac{1}{|\mathcal{S}_{t-1}|} \sum_{s \in \mathcal{S}_{t-1}} d(\mathbf{h}_c, \mathbf{h}_s)$ 
9:      $\mathcal{D}_{\text{query}}(c) \leftarrow \frac{1}{|\mathcal{C}_{t-1}| - 1} \sum_{j \in \mathcal{C}_{t-1} \setminus \{c\}} d(\mathbf{h}_c, \mathbf{h}_j)$ 
10:   end for
11:   // Diversity-Representativeness score
12:   for  $c \in \mathcal{C}_{t-1}$  do
13:      $r_1(c) \leftarrow \text{rank of } \mathcal{D}_{\text{ref}}(c) \text{ in descending order}$ 
14:      $r_2(c) \leftarrow \text{rank of } \mathcal{D}_{\text{query}}(c) \text{ in ascending order}$ 
15:      $\rho(c) \leftarrow \frac{r_1(c) + r_2(c)}{2}$ 
16:   end for
17:   // Select optimal candidate
18:    $s_t \leftarrow \arg \min_{c \in \mathcal{C}_{t-1}} \rho(c)$ 
19:    $\mathcal{S}_t \leftarrow \mathcal{S}_{t-1} \cup \{s_t\}, \mathcal{C}_t \leftarrow \mathcal{C}_{t-1} \setminus \{s_t\}$ 
20: end for
21: return  $\mathcal{S}_k$ 

```

figuration are often more complex and subtle, as the datasets include a diverse range of image contents and exhibit notable retouching inconsistencies. The same user’s stylistic adjustments may vary significantly across images, even when they share similar visual attributes. Consequently, personalization in this setting requires a larger number of reference samples to effectively capture the user’s underlying retouching patterns. In our experiments, we sampled a few representative reference images from the training split (see Section Section 8 for details), while using the same test split for evaluation as defined in the original benchmark [42].

8. Reference Samples Selection

In practice, users typically provide a set of representative reference image pairs that share similar visual characteristics with the images they intend to retouch. To simulate this behavior in our experiments and ensure that the selected references contain information relevant to the test images, we adopt a color–tone distribution–guided sampling strategy to partition each benchmark into reference and test splits.

Specifically, we represent each image using histogram

features extracted in the CIE–Lab color space. For each input image x_i , we compute a 1D histogram of the L channel with 16 bins to capture the tonal distribution, and a 2D joint histogram of the ab chromatic channels with 16×16 bins (256 bins in total) to model color variation. These are concatenated to form a unified color–tone feature vector $h_i \in \mathbb{R}^{272}$:

$$h_i = [H_L(x_i); H_{ab}(x_i)] \quad (4)$$

We then apply the sampling strategy described in Algorithm 1 to select references that are both representative and diverse. At each iteration, every candidate image is evaluated based on two complementary criteria: (i) its average distance to the already selected references, which encourages diversity, and (ii) its average distance to the remaining unselected candidates, which promotes representativeness. These two scores are combined using a simple rank-based fusion to obtain a single selection score for each image. The process is repeated in a greedy manner until the desired number of reference samples is obtained. The Chi-square distance is used to measure similarity between histogram features, as it effectively captures perceptual differences in color and tone distributions.

We employ this reference sampling procedure across all three benchmarks. The same sampled references are consistently used for evaluating both baseline methods and our proposed model to ensure fairness. For each benchmark, we first sample the maximum number of references: 4, 6, and 100 pairs for VCIRB, PPR10K-groups, and the MIT-FiveK/PPR10K datasets, respectively and then derive smaller subsets by selecting the first k references for experiments with fewer exemplars.

9. Additional Qualitative Results

We provide additional qualitative results demonstrating the visual effectiveness and generalization capability of our method across different personalization scenarios. We provide additional qualitative results to complement the main paper. Figure 7 shows personalization results from a single reference pair, while Figure 8, Figure 9, and Figure 10 illustrate our model’s performance on the PPR10K-groups benchmark with one, three, and six reference exemplars, respectively. Furthermore, Figure 11 presents additional photorealistic style transfer comparisons across diverse content and style references.

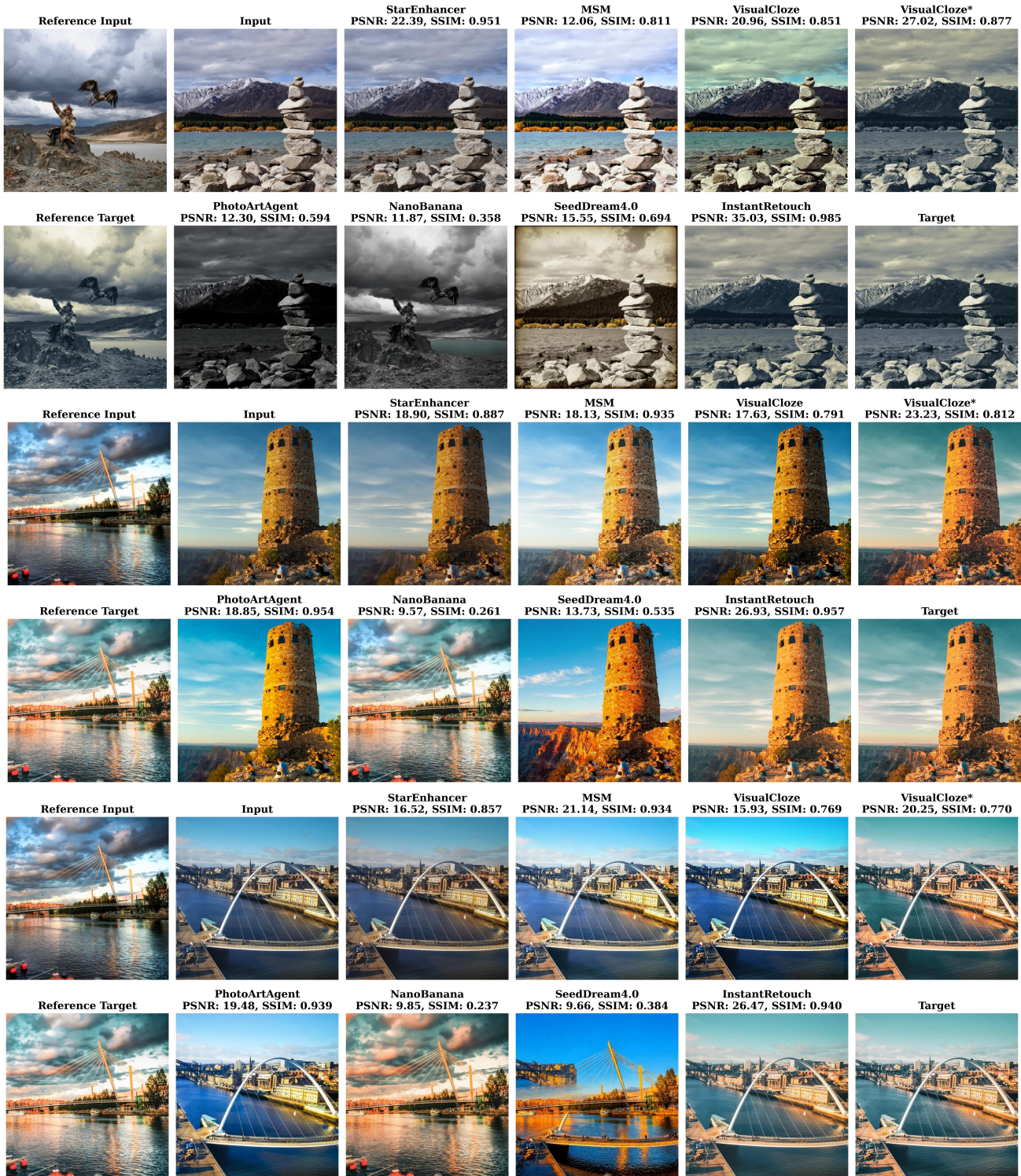


Figure 7. VCIRB single reference personalized image retouching qualitative result comparisons

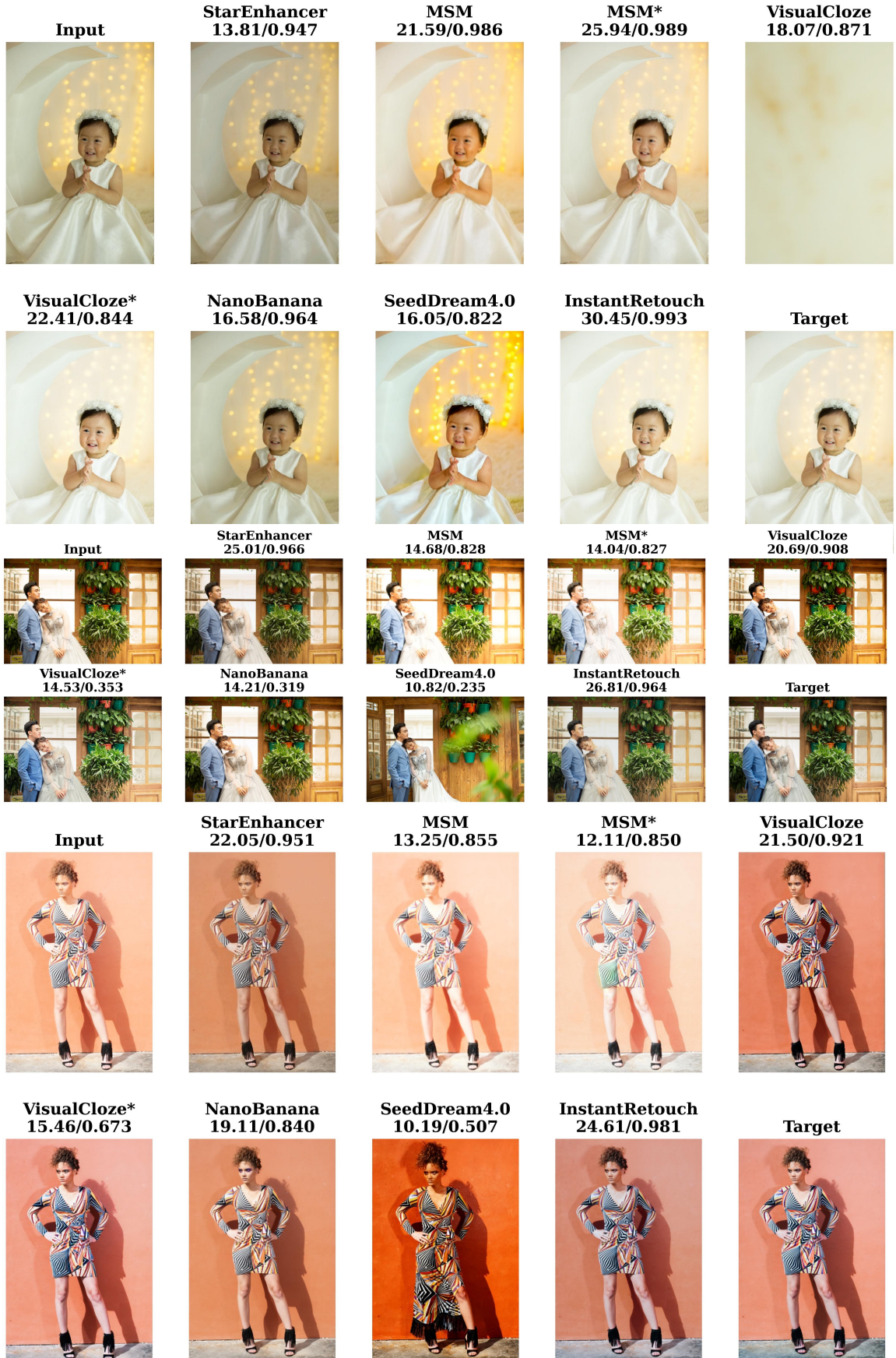


Figure 8. PPR10k-groups singe reference personalized image retouching qualitative result comparisons

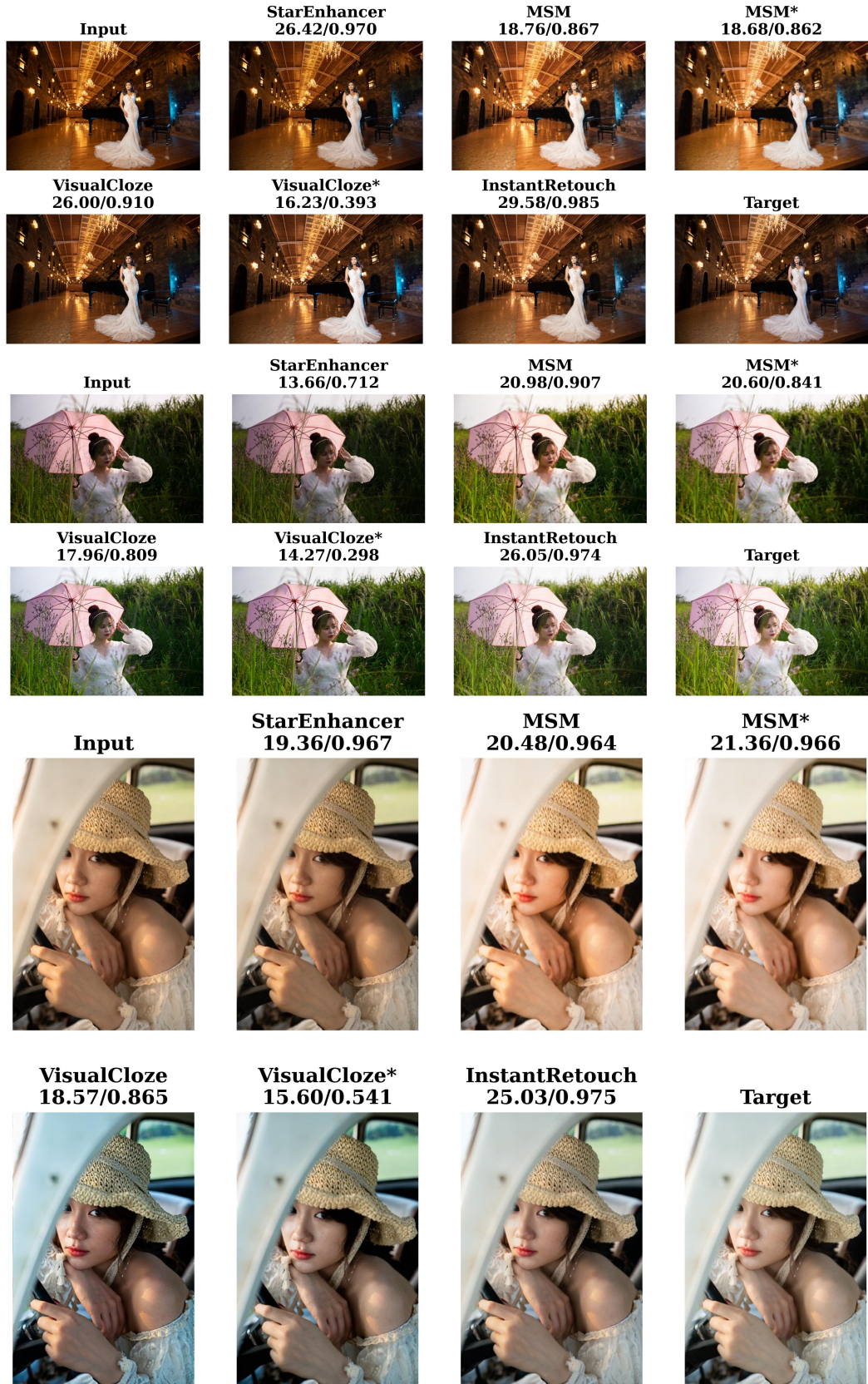


Figure 9. PPR10k-groups three references personalized image retouching qualitative result comparisons

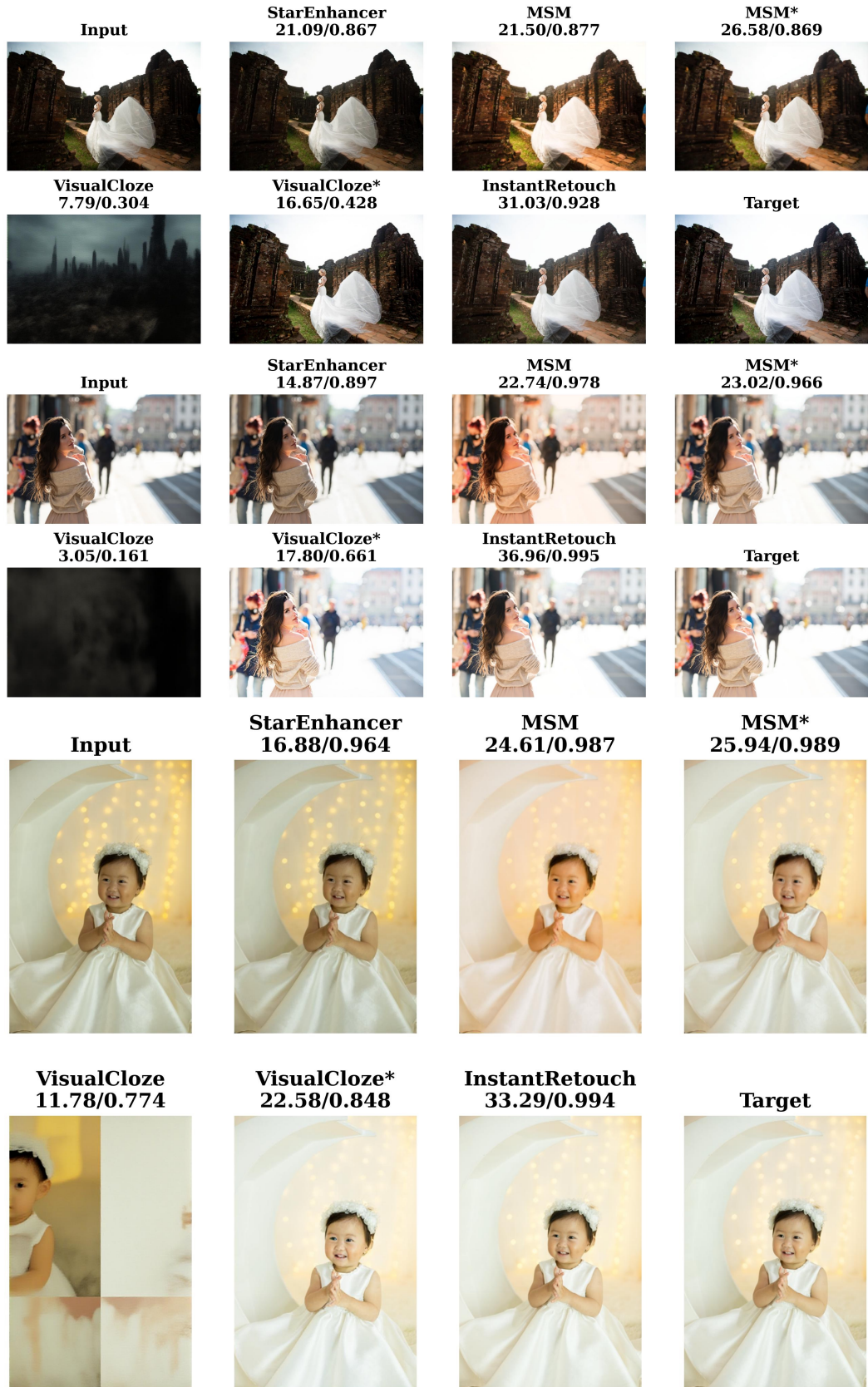


Figure 10. PPR10k-groups six references personalized image retouching qualitative result comparisons

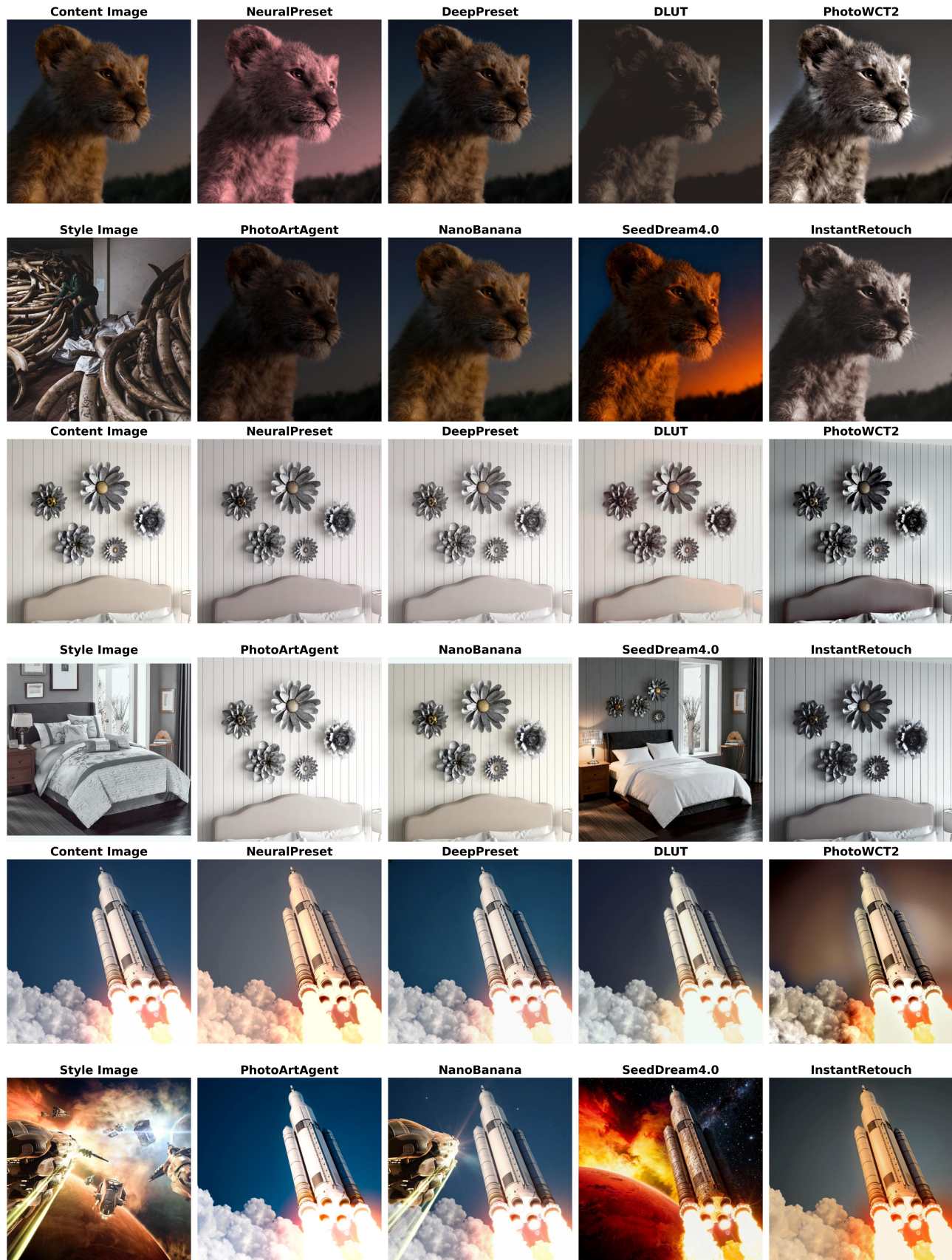


Figure 11. Photorealistic style transfer qualitative result comparisons